JOURNAL OF CATALYSIS 99, 461–471 (1986)

Characterization of NH_3/Fe Catalytic Systems by Laser Raman Spectroscopy

HONG-BIN ZHANG[1] AND G. L. SCHRADER[2]

Department of Chemical Engineering, Iowa State University, Ames, Iowa 50011

Received May 3, 1985; revised January 21, 1986

Laser Raman spectra of species adsorbed on doubly promoted fused iron catalysts were obtained under static and flowing atmospheres of NH_3 and $1N_2/3H_2$. The spectra provided new information about the nature of the surface species involved in iron–hydrogen, iron–nitrogen, and nitrogen–nitrogen bonding. Assignment of the Raman bands included: 1951 and 1902 cm^{-1} for the Fe—H stretch due to H(a); 1940 and 2040 cm^{-1} for the N≡N stretch due to N_2(a); 1090 cm^{-1} for the Fe≡N stretch due to N(a); 895 cm^{-1} for the Fe=N stretch due to NH(a); 500 cm^{-1} for the Fe—N stretch due to NH_2(a); 465 and 410 cm^{-1} for the Fe—N stretch due to N_2(a); and 140 cm^{-1} for the Fe—N stretch due to NH_3(a). *In situ* studies and studies performed at room temperature indicated that dehydrogenation of NH_3(a) to NH(a) or N(a) did not occur extensively for catalysts which had been reduced by H_2 or for catalysts which were actually functioning for NH_3 decomposition. N_2(a) and H(a) were the dominant chemisorbed species on the surface of the functioning catalyst. The Raman results were consistent with an associative mechanism for ammonia synthesis or decomposition:

$$2NH_3(a) \overset{-(6-x-y)H(a)}{\rightleftharpoons} NH_x(a) + NH_y(a) \rightleftarrows N_2H_{x+y}(a) \overset{-(x+y)H(a)}{\rightleftharpoons} N_2(a) \rightleftarrows N_2(g),\ (x, y = 1 \text{ or } 2).$$

I. INTRODUCTION

Ammonia synthesis catalysts have been investigated extensively since their discovery nearly 80 years ago: general rate expressions have been determined by kinetic studies, and various instrumentation techniques have provided information about the structure and composition of active catalysts. However, these studies have generally been unable to directly distinguish various mechanisms which have been proposed for ammonia synthesis or decomposition reactions. Characterization of the catalytic systems involved in ammonia synthesis using vibrational spectroscopy offers the potential for providing new information about the nature of adsorbed species and intermediates on the surfaces of the catalysts; a useful elucidation of the mechanism of the ammonia synthesis reaction could then result.

Previous vibrational spectroscopic studies have largely relied on the use of infrared spectroscopy to examine NH_3 and N_2/H_2 adsorbed on iron catalysts. Nakata and Matsushita (1) observed NH_2(a) and NH(a) species on a silica-supported iron catalyst. Brill *et al.* (2) detected NH(a) species which were assigned to a hydrazine-like surface species adsorbed on a magnesia-supported iron catalyst. Tamaru *et al.* (3, 4), using Fourier transform infrared spectroscopy, observed bands at 2200, 2050, and 500 cm^{-1} for a Fe/MgO catalyst which had been used for ammonia decomposition; the peaks at 2200 and 2050 cm^{-1} were assigned to the N≡N stretch of adsorbed N_2 and the 500-cm^{-1} peak was assigned to a Fe—N (—NH_x) stretch.

However, the application of infrared spectroscopy to the study of ammonia synthesis encounters serious difficulties due to strong absorption by the catalysts. This ob-

[1] Permanent address: Department of Chemistry and Institute of Physical Chemistry, Xiamen University, China.

[2] To whom correspondence should be addressed.

0003-9517/86 $3.00

scures a considerable portion of the infrared spectrum, particularly the lower wavenumber region in which metal–nitrogen vibrations would be expected to be observed. In contrast, Raman spectroscopy is an attractive choice for characterization of ammonia synthesis and decomposition reactions using iron catalysts for several reasons. First, the iron catalysts have relatively simple—and often very weak—Raman bands in the metal–nitrogen vibrational region (clearly evidenced for the reduced catalyst). Second, the iron–nitrogen bond has a rather strong Raman scattering "cross section," thereby indicating the potential for good sensitivity for adsorbed species and intermediates which are involved in such bonding. Recently, Tsai, *et al.* (*5, 6*) reported Raman spectra for N_2/H_2 adsorption and NH_3 decomposition on iron catalysts. A strong band at 1940 cm^{-1} was assigned to a chemisorbed N_2 species and several peaks at low wavenumbers were attributed to iron–nitrogen bonds (N_2(a) or N(a) species). These authors inferred from their experimental results that chemisorbed N_2 rather than N(a) and NH(a) was the dominant species under typical ammonia synthesis conditions.

However, the assignment of these bands to specific iron–nitrogen complexes was not thoroughly established by these investigations. In the present paper, *in situ* laser Raman spectroscopy has been applied to the investigation of adsorption on a doubly promoted iron catalyst. The Raman spectra of the adsorbed species under various decomposition (NH_3) and synthesis (N_2/H_2) conditions have been related to the mechanisms for the decomposition and synthesis of ammonia on iron catalysts.

II. EXPERIMENTAL PROCEDURE

Raman spectra were recorded with a Spex Industries 1403 Raman spectrometer. The 514.5-nm line from a Spectra Physics Model 164 argon ion laser was used as the excitation source with an intensity of approximately 400 mW measured at the source. Slit width settings correspond to a resolution of 4 cm^{-1}. The spectrometer was interfaced with a Nicolet 1180E data system for recording spectra. Spectral accumulation was necessary to obtain spectra; up to 60 scans were accumulated in some cases to obtain an acceptable signal-to-noise ratio.

Spectra were obtained in several controlled atmosphere cells, such as have been previously discussed by Schrader and Hill (*7*) and Cheng *et al.* (*8*).

A doubly promoted, fused iron catalyst was used in this investigation. This catalyst is typical of industrial ammonia synthesis catalysts and was produced by heating a mixture of magnetite (Fe_3O_4), K_2O (1%), and Al_2O_3 (3%) in an electric are furnace to 1500°C. Prior to the Raman investigations, samples were prereduced in a quartz spectroscopic cell by a flow of purified H_2 at: 120°C for 2 h, 250°C for 2 h, 350°C for 8 h, and finally 450°C for a minimum of 24 h. The surface area of this catalyst was 15 m^2/g.

Raman spectra of chemisorbed species on the catalyst were obtained by exposing the samples to flowing and static NH_3, $1N_2$/$3H_2$, or N_2. Gaseous H_2 (Matheson, UHP, 99.999%) and N_2 (air product, 99.9%) were purified by passing through a Deoxo purifier and then through a 5-Å molecular sieve trap. Ammonia (Matheson, dehydrous) was purified by passing through a 5-Å molecular sieve trap. Spectra were obtained at atmospheric pressure; a series of temperature variations was examined. Spectra were recorded *in situ* as well as after rapid cooling to room temperature.

III. EXPERIMENTAL RESULTS

A. Raman Spectra of the H_2-Reduced Catalyst

The doubly promoted iron catalyst was reduced prior to obtaining Raman spectra of the adsorbed species. During industrial ammonia synthesis, reduction of the iron catalyst occurs extensively, and the reduc-

tion pretreatment described under Experimental Procedure effectively represents this process.

The Raman spectrum of the fused iron catalyst in the region of 1850–2350 cm^{-1} after reduction by H_2 at 450°C for 48 h and cooling to room temperature is shown in Fig. 1a. Bands are observed at 1870, 1902, 1954, 2165, and 2331 cm^{-1}. The spectrum shown in Fig. 1b was obtained *in situ* under the conditions of 400°C and atmospheric pressure in a flow of H_2; only three bands are apparent at 1902, 1951, and 2331 cm^{-1}. Kavtaradze and Sokolova (*9*) have reported that the adsorption of hydrogen on alumina-supported iron, cobalt, and nickel is dissociative. The infrared bands of the corresponding surface hydrides are in the range of 1850–1940 cm^{-1}. According to Kaesz and Saillant (*10*), and Johnson and Lewis (*11*), the M—H stretching frequency for terminally bonded hydrogen in most transition-metal molecular clusters falls in the range of 1850–2200 cm^{-1}, and the intensities of the vibrations are very sensitive to temperature. Consequently, the bands 1870, 1902, and 1951 (1954) cm^{-1} may be reasonably assigned to metal–hydrogen vibrations. The 2331-cm^{-1} peak is due to the stretching mode of free dinitrogen existing in the atmosphere associated with the general sample compartment region of the spectrometer. For the 2160-cm^{-1} peak, a satisfactory assignment is not possible at present, although the importance of this peak under *in situ* functioning-catalyst conditions is doubtful.

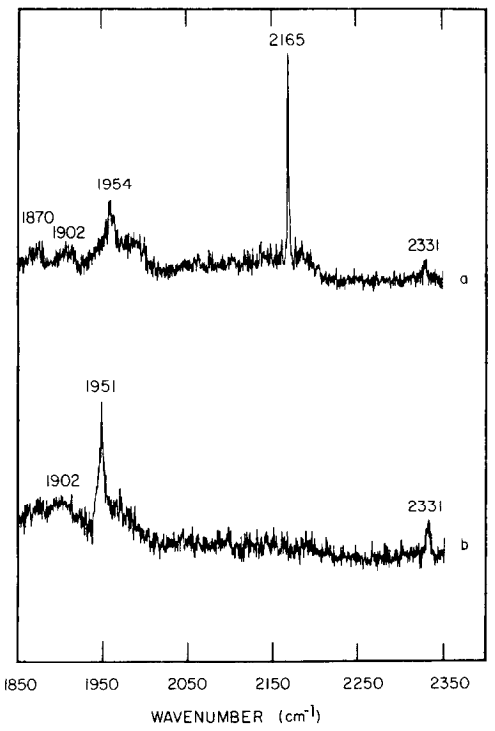

FIG. 1. Raman spectra of the doubly promoted fused iron catalyst after reduction by flowing H_2 at 450°C for 48 h in the region of 1850–2350 cm^{-1}: (a) taken at room temperature and under static H_2 atmosphere; (b) taken *in situ* at 400°C and in flowing H_2.

Figures 2a and b are the Raman spectra of the same catalyst in the region of 400–1200 cm^{-1} under static conditions (room temperature and static H_2) and *in situ* conditions (400°C and flowing H_2), respectively. Except for the 589-cm^{-1} peak, which has been identified to be due to the Si—H stretch involving hydrogen atoms adsorbed on the quartz window of the sample cell (*12*), there are no observable Raman peaks for the sample; in addition, the "background" signal for the sample is low.

B. Raman Spectra of NH_3/Fe and N_2/H_2/Fe Systems

Raman spectra were obtained for the adsorption of NH_3 and N_2/H_2 on the doubly promoted iron catalysts. The assignment of the Raman bands to specific adsorbed species was accomplished by establishing the relative concentration of the adsorbed species present on the catalyst surface under specific experimental conditions; variations in feed gases and their flow rates, temperature effects, competitive adsorption, and desorption were all effective in assisting in the assignment.

Figures 3a and b are the 1850–2350 cm^{-1} region of the Raman spectra for species adsorbed respectively on the doubly promoted fused iron catalyst after 4 h of NH_3 decomposition (in a flow of NH_3) and synthesis (in a flow of $1N_2/3H_2$) at 400°C. It can

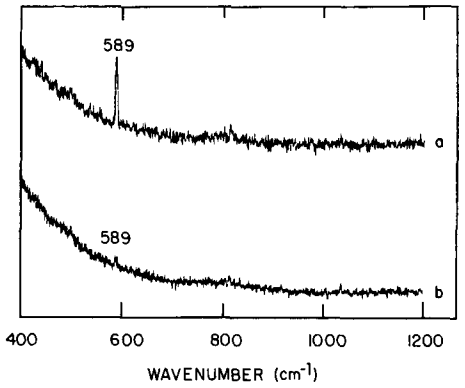

FIG. 2. Raman spectra of the doubly promoted fused iron catalyst after reduction by flowing H_2 at 450°C for 48 h in the region of 400–1200 cm^{-1}: (a) taken at room temperature and under static H_2 atmosphere; (b) taken *in situ* at 400°C and in flowing H_2.

be seen that their major spectral features are similar although some differences in the relative concentration of the various adsorbed species are present. Common bands are observed at 1870, 1902, 1940, 1951, 2040, 2150 (2160), and 2331 cm^{-1}. It has generally been accepted that a considerable amount of chemisorbed hydrogen, H(a), exists on the surface of iron catalyst under the conditions for ammonia decomposition and synthesis. In comparing the spectra for NH_3/Fe and $1N_2/3H_2$/Fe with that for H_2/Fe (Fig. 1a), the bands at 1870, 1902, and 1951 cm^{-1} may reasonably be attributed to stretching vibrations of Fe—H bonds, while the 1940- and 2040-cm^{-1} bands are probably due to species concerned with chemisorbed nitrogen. The N≡N stretching frequencies in most transition metal–dinitrogen complexes or molecular cluster are shifted toward lower energies. According to Collman and Hegedus (*13*), $\nu_{N\equiv N}$ for single end-on η^1–N_2 complexes or molecular clusters falls in the region of 2200–2000 cm^{-1}, and $\nu_{N\equiv N}$ for double end-on η^2–N_2 complexes or molecular clusters may be as low as 1660 cm^{-1} (reaching down to 1282 cm^{-1} in a Ti_3-molecular cluster (*14*)). Consequently, the 1940- and 2040-cm^{-1} bands may be assigned to N≡N stretches for chemisorbed N_2(a) species with different coordination modes on the surface of the catalyst.

The 350–1150 cm^{-1} region of the Raman spectra for species adsorbed on the doubly promoted fused iron catalyst after 4 h of NH_3 decomposition (in a flow of NH_3) and after NH_3 synthesis (in a flow of a mixture of $1N_2/3H_2$) at 400°C are shown in Fig. 4a and b, respectively. Bands were observed at 500 cm^{-1} for NH_3 decomposition (Fig. 4a) and at 410 and 465 cm^{-1} for NH_3 synthesis (Fig. 4b). These bands are due to vibrations associated with iron–nitrogen bonds, corresponding to NH_x(a) or N_2(a) species, respectively.

The previously described experiments would be expected to produce a relatively high concentration of species associated with ammonia decomposition and synthesis. Raman spectra were also obtained for pure N_2 adsorption on reduced catalysts. Samples of the catalyst (in powder form

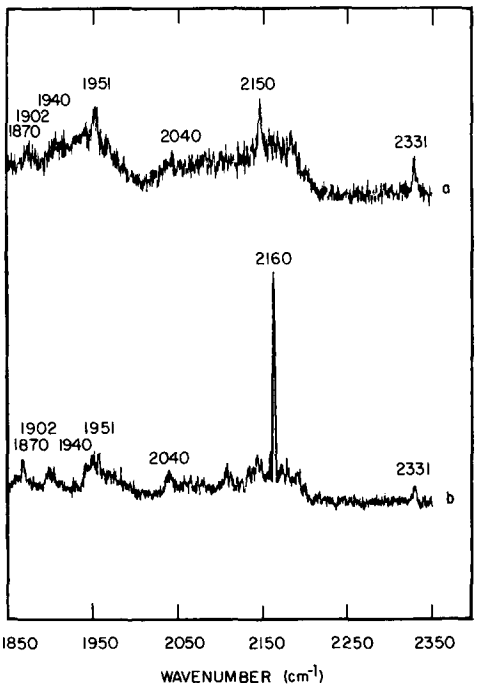

FIG. 3. Raman spectra of species adsorbed on the doubly promoted fused iron catalyst at room temperature in the region of 1850–2350 cm^{-1}: (a) taken after 4 h of NH_3 decomposition at 400°C; (b) taken after 4 h of NH_3 synthesis at 400°C.

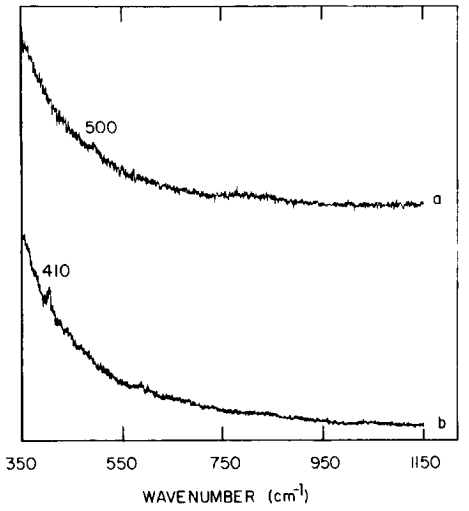

FIG. 4. Raman spectra of species adsorbed on the doubly promoted fused iron catalyst at room temperature in the region of 350–1150 cm^{-1}: (a) taken after 4 h of NH_3 decomposition at 400°C; (b) taken after 4 h of NH_3 synthesis at 400°C.

without being pressed into a wafer) were reduced by purified H_2 in a quartz cell according to the previously described methods, and subsequently exposed to flowing N_2 at 500°C for 1 h. The resulting Raman spectra is quite different from those discussed for NH_3 decomposition and synthesis (Fig. 5a). The dominant spectral feature is a band at 1090 cm^{-1} although the unusually broad nature of this band makes this wavenumber designation approximate. According to Chatt and Nakamoto (*15, 16*), stretching vibrations for most metal–nitrogen triple bonds occur in the 1000- to 1200-cm^{-1} region. Under the treatment conditions for this catalyst this would be a reasonable assignment, specifically for the stretching vibration of Fe≡N species involving atomically adsorbed N. The Raman spectrum of this sample gives very limited indication that other species are present, although another band can be observed near 895 cm^{-1}. The intensity of this band can be dramatically increased by treating the sample under a flow of H_2 at 500°C for 30 min (Fig. 5b); at the same time, the intensity of the 1090-cm^{-1} band is dramatically decreased. The hydrogenation conditions apparently convert the atomically adsorbed N species to hydrogenated —NH_x species. Interestingly, the intensity of the 895-cm^{-1} band is very dependent on the time of exposure to hydrogen; it is conceivable that the concentration of primary hydrogenated species, NH(a), would pass through a maximum as hydrogenation proceeds to form NH_2(a) species. Such behavior is shown in Fig. 5c, where after hydrogen treatment at 500°C for another 40 min, the 895-cm^{-1} band intensity is greatly decreased, implying that most of the primary hydrogenated species have been converted to highly hydrogenated species, NH_2(a) and NH_3. These results substantiate the assignment of the 895-cm^{-1} band to NH_x(a) species: it is reasonable to assign the 895-cm^{-1} band to

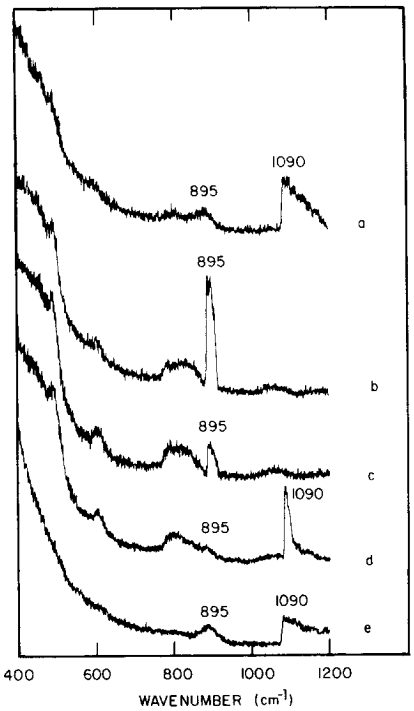

FIG. 5. Raman spectra (obtained at room temperature) of species adsorbed on the doubly promoted fused iron catalyst which was reduced by H_2 followed by successive treatments with: (a) N_2 at 500°C for 1 h; (b) H_2 at 500°C for 30 min; (c) H_2 at 500°C for an additional 40 min; (d) NH_3 decomposition at 450°C for 2 h, followed by evacuation under a dynamic vacuum of 10^{-2} to 10^{-3} Torr at 450°C for 50 min; (e) $10N_2/1H_2$ at 500°C for 40 min, followed by exposure to flowing N_2 at 500°C for 20 min.

the Fe=N stretching vibration of NH(a). It is interesting to note that the 1090-cm^{-1} band can also be detected for ammonia decomposition experiments where the sample has been evacuated (10^{-2} to 10^{-3} Torr for 50 min) at 450°C. The result of such an experiment is shown in Fig. 5d. This spectrum may be interpreted in terms of the removal of dinitrogen and hydrogen from the surface, accompanied by the dehydrogenation of NH_2(a) and NH_3(a) species; an increased concentration of NH(a) and N(a) species would then result.

Since the catalyst powder samples were positioned in contact with the inner surface of the quartz window in the previous experiments, the observed spectra also involved some contribution from the quartz window. Blank tests (without catalyst sample) have proved that the bands observed at 491, 602, 800 (broad), 1060 (broad and weak) cm^{-1} are all due to vibrations of Si—O bonds of the quartz window. As described previously by Cheng *et al.* (*8*), positioning of the sample a few millimeters away from the optical window reduces the intensity of light scattered by the quartz window. Figure 5e shows the result of pressing the catalyst into a wafer; the sample was then prereduced by purified H_2, sequentially exposed at 500°C to flowing $10N_2/1H_2$ for 40 min and to flowing N_2 for 20 min, and finally cooled to room temperature in a N_2 atmosphere. Only the 895- and 1090-cm^{-1} Raman bands of adsorbed species are observed. In an EELS investigation of NH_3/Fe(110) under conditions of ultrahigh vacuum and low temperature performed by Erley and Ibach (*17*), energy losses at 500, 880, and 1020 cm^{-1} were observed after the sample was exposed to 3 Langmuirs ammonia and heated to 315 K. According to Tamaru *et al.* (*3, 4*) and our experimental results, however, the ascription of the loss at 500 cm^{-1} to atomically adsorbed nitrogen and of the losses at 880 and 1020 cm^{-1} to atomically adsorbed hydrogen proposed by these workers may not be justifiable. Our assignment of these Raman bands at 500, 895, and 1090 cm^{-1} is consistent with the corresponding bond energy values inferred by Bozso *et al.* (*21*), who estimated the following bond energy values: 140 kcal/mol for Fe≡N due to N(a), 100 kcal/mol for Fe=N due to NH(a), 65 kcal/mol for Fe—N due to NH_2(a), and 10 kcal/mol for Fe—N due to NH_3(a).

In order to obtain information about the nature of the Fe—N bond for NH_3(a), the 130–330 cm^{-1} region of the spectrum has also been investigated. Figure 6 shows the results of such a set of observations. A peak assignable to Fe—N stretching for NH_3(a) was observed at 140 cm^{-1} for a H_2-reduced sample (Fig. 6b) which had been exposed for 2 h to NH_3 at room tempera-

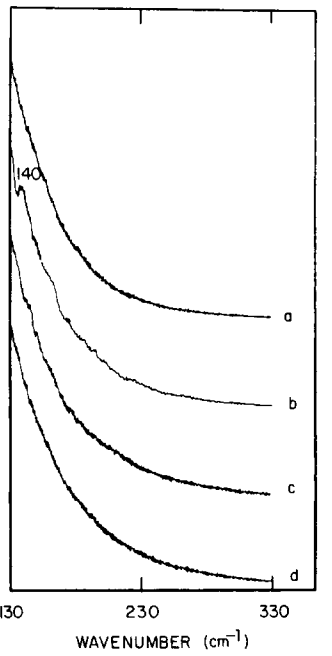

FIG. 6. Raman spectra of species adsorbed on the doubly promoted iron catalyst in the region of 130–330 cm^{-1}: (a) taken on a sample of the catalyst after 48 h of H_2 prereduction at 450°C and then cooling to room temperature; (b) taken after 2 h of exposure of the H_2-prereduced catalyst to gaseous NH_3 at room temperature and under atmospheric pressure; (c) taken after 3 h of NH_3 decomposition at 400°C and then cooling in flowing NH_3 to room temperature; (d) taken *in situ* at 400°C under reaction conditions for NH_3 decomposition; NH_3 flowing at feed rate of 3000 ml gas at 25°C, 1 atm/cm^3 catalyst h.

ture. However, this peak was not observed under actual reaction conditions for NH_3 decomposition at 400°C (Fig. 6d) or after subsequent cooling to room temperature (Fig. 6c). This indicates that the concentration of NH_3(a) on the working surface of the catalyst is quite low under steady state conditions for NH_3 decomposition.

C. In Situ Raman Spectra of the Functioning Catalyst

The previously discussed spectra (except Figs. 1b, 2b, 6d) were obtained at room temperature; in some cases this involved considerable cooling of the sample so that the reaction conditions were perturbed. *In situ* studies were performed to confirm the presence of the previously discussed species at high temperature.

Shown in Figs. 7 and 8 are the Raman spectra (both at 400°C under atmospheric pressure) for the doubly promoted iron catalyst after exposure to NH_3 (ammonia decomposition conditions) and after exposure to a mixture consisting of $3H_2/1N_2$ (ammonia synthesis conditions). From the observed results in the region of 1850–2350 cm^{-1} (Fig. 7), it can be seen that the Fe—H peaks at 1902 and 1951 cm^{-1} and the N≡N peaks at 1940 and 2040 cm^{-1} were observable under *in situ* conditions at 400°C. There is little difference in the positions of the Raman peaks for the adsorbed species for spectra 7a and 7b, although the relative concentrations of the various adsorbed species on the surfaces may be somewhat different; however, the bands in the 2150-cm^{-1} region, which were present in the spectra taken at room temperature and under static conditions, were absent from the *in situ* spectra. For the spectra of the 400- to 1200-cm^{-1} region (Fig. 8) obtained under the same conditions, only those peaks assignable to Fe—N (N_2(a)) were apparent; the Fe—N (NH(a)) peak at 890 cm^{-1} and the

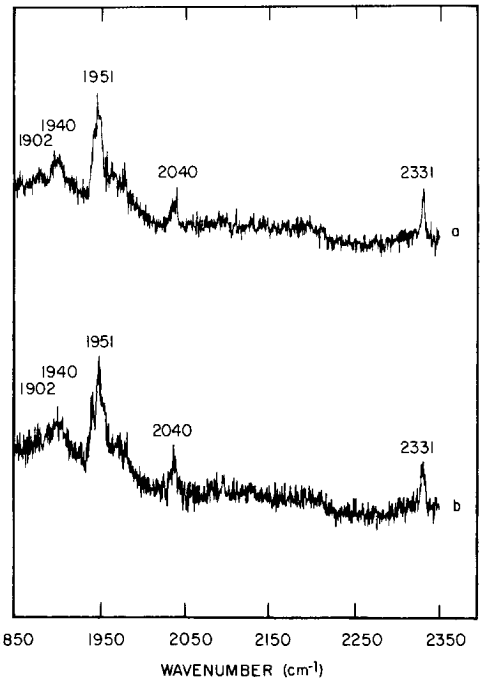

FIG. 7. *In situ* Raman spectra at 400°C in the region of 1850–2350 cm^{-1} of intermediates adsorbed on doubly promoted fused iron catalyst under conditions of: (a) NH_3 at feed rate of 6000 ml gas at 25°C, 1 atm/cm^3 catalyst h; (b) $1N_2/3H_2$ gaseous mixture at feed rate of 15,000 ml gas at 25°C, 1 atm/cm^3 catalyst h.

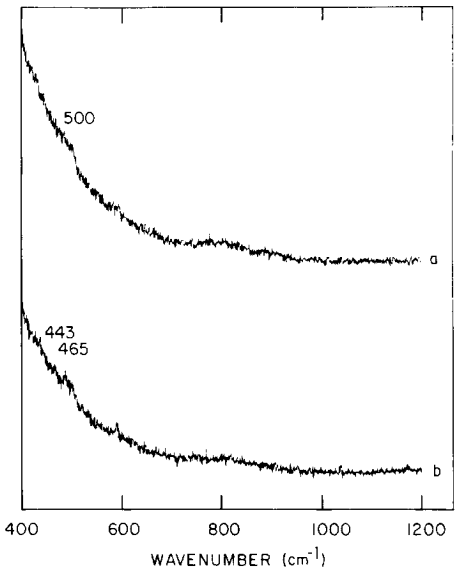

FIG. 8. *In situ* Raman spectra at 400°C in the region of 400–1200 cm^{-1} of intermediates adsorbed on doubly promoted fused iron catalyst under conditions of: (a) NH_3 at feed rate of 6000 ml gas at 25°C, 1 atm/cm^3 catalyst h; (b) $1N_2/3H_2$ gaseous mixture at feed rate of 15,000 ml gas at 25°C, 1 atm/cm^3 catalyst h.

Fe—N (N(a)) peak at 1090 cm^{-1} were not observable.

From these results, it can be inferred that the species associated with the 1940- and 2040-cm^{-1} peaks with the 1902- and 1951-cm^{-1} peaks—respectively, $N_2(a)$ and H(a)—were the predominant intermediates on the surface for actual steady-state ammonia decomposition/synthesis conditions. Neither NH(a) (890 cm^{-1}) nor N(a) (1090 cm^{-1} were the major species under these circumstances.

IV. DISCUSSION OF RESULTS

All Raman bands observed for these studies and their assignments are summarized in Table 1. The results of this Raman spectroscopic study have important applications for the general understanding of the mechanisms of ammonia decomposition and synthesis reactions.

Previous studies of the adsorption of NH_3 by electron spectroscopy have shown that when ammonia is adsorbed on polycrystalline iron surfaces, the molecular form is predominant at 85 K. When samples are warmed to 290 K, two types of species are observed. These were considered to be dissociated species, N(a) and NH(a), and molecular species; the dissociated species were believed to be dominant (*18*). Very similar species were observed at higher temperature on the α-Fe(III) surface of a single crystal. The dissociated species appeared to be identical to that obtained from the dissociative adsorption of nitrogen, implying that extensive dehydrogenation of ammonia occurs.

TABLE 1

Assignment of Raman Bands for Adsorbed Species Associated with Ammonia Synthesis and Decomposition

Band position (cm^{-1})	Assignment
1951, 1902	Stretching of Fe—H for H(a)
1940, 204	Stretching of N≡N for $N_2(a)$
1090	Stretching of Fe≡N for N(a)
895	Stretching of Fe=N for NH(a)
500	Stretching of Fe—N for $NH_2(a)$
465, 443, 410	Stretching of Fe—N for $N_2(a)$
140	Stretching of Fe—N for $NH_3(a)$

However, this information was obtained under conditions much removed from actual reaction conditions, and significant differences could be expected with data obtained at *in situ* reaction conditions. The results obtained from our studies provide new information about the mechanisms for ammonia decomposition and synthesis. It has been suggested that the energy level of N(a) is the lowest in the thermochemical kinetics profile for NH_3 synthesis and decomposition (*20–22*). If nitrogen recombination were the rate-controlling step in ammonia decomposition, atomically chemisorbed nitrogen, N(a), would be the most abundant reaction intermediate. However, our experimental results have shown that the chemisorbed dinitrogen $N_2(a)$ and H(a), rather than N(a) or NH(a), are the predominant chemisorbed species under actual reaction conditions for NH_3 decomposition. This probably was due to the fact that the iron catalyst samples—either strongly reduced by pure H_2 or working under practical reaction conditions for NH_3 decomposition—were nearly saturated by chemisorbed H and dissolved H present in the bulk. $NH_x(a)$ (where $x = 0, 1, 2$) species and H(a) are involved in the rapid equilibrium

$$NH_3(g) \rightleftarrows NH_3(a) \rightleftarrows H(a) + NH_2(a) \rightleftarrows 2H(a) + NH(a) \rightleftarrows 3H(a) + N(a)$$

so that the existence of a great amount of H(a) and H in the bulk would inhibit dehydrogenation of $NH_3(a)$ to N(a) or NH(a). Ertl (*23*) and Huber (*24*), considering the reverse reaction, i.e., NH_3 synthesis, have investigated the surface concentration of atomic nitrogen on the α-Fe(III) surface under catalyst working conditions and found that the steady-state concentration of surface N(a) becomes very small at 310°C in the presence of a stoichiometric mixture (450 Torr H_2 and 150 Torr N_2). Similar be-

havior was observed in the photoelectron spectroscopic studies by Gay *et al.* (*19*) for the adsorption of ammonia on iron: extensive dehydrogenation occurred only at low coverages, but associative adsorption dominated at high coverages. These investigators also examined the effect of preadsorbed hydrogen on the chemisorption of ammonia and concluded that the major surface species was clearly the associated species, particularly for higher coverages on the α-Fe(III) surface. Only on the surfaces of iron catalysts which experienced high exposure to pure N_2 was dissociatively adsorbed N(a) the major chemisorbed species (see Figs. 5a, e).

The existence of molecularly chemisorbed nitrogen, $N_2(a)$, and its partially hydrogenated derivatives on the surfaces of ammonia synthesis iron catalysts has been inferred by several investigators. The FIM investigation conducted by Schmidt (*25*) indicated the presence of N_2H^+, $N_2H_2^+$, and $N_2H_3^+$ as some of the major species. The presence of molecularly adsorbed $N_2(a)$ on iron catalysts was also shown by Toyoshima (*26*) from his thermal-desorption rate experiment and the exchange reaction rate between $^{28}N_2$ and $^{30}N_2$ on iron catalysts in the presence of H_2 at 350–450°C. On clean α-Fe(III) surfaces under high vacuum and low temperature, a linearly coordinated $N_2(a)$ (γ-state) and a flat-lying coordinated $N_2(a)$ (α-state) have recently been identified by Grunze *et al.* (*27*) using XPS and HREELS. Our results for *in situ* reaction conditions for both ammonia decomposition and synthesis have also shown that nitrogen and hydrogen may exist in more than one adsorption state on the surface of the fused iron catalyst. Among them, the states corresponding to the Raman peaks at 1940 and 2040 cm^{-1} appeared to be the major molecularly chemisorbed nitrogen-containing species, $N_2(a)$. Both the Raman peak at 2040 cm^{-1} and the IR band at 2050 cm^{-1} reported by Tamaru *et al.* (*4*) are probably attributed to a common stretching vibration mode of N≡N, which has a single-end-on-plus-multiple-side-on coordination, thus making the vibrational mode active in the infrared as well as the Raman. Since no IR band in the 1940-cm^{-1} region has been observed, it is probable that the coordination mode of chemisorbed $N_2(a)$ associated with this Raman peak is a flat-lying-double-end-on-bridge-type, as has been suggested and discussed by Tsai *et al.* (*5, 28, 29*). Comparatively high concentrations of $N_2(a)$ in the two chemisorption states on the working surface of the catalyst at 400°C (Fig. 7) imply that these species were not easily replaced by molecules of NH_3 and that rather high activation energies were involved in their desorption. The 2200-cm^{-1} IR band observed by Tamaru (*4*) might result from a weak terminal adsorption mode of $N_2(a)$, which has not been found in our *in situ* Raman investigation at 400°C probably because of a low stationary concentration of this state on the surface of the working catalyst. It is conceivable that the transformation from one of these states of adsorbed dinitrogen, $N_2(a)$, to another one may readily occur in the following sequence of steps under actual reaction conditions:

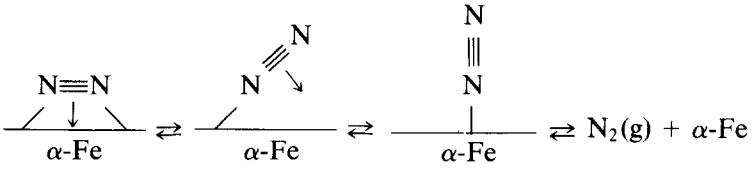

Among these adsorbed dinitrogen species, the $N_2(a)$ species with the flat-lying-double-end-on-bridge-type coordination mode would be the most favorable for the activa-

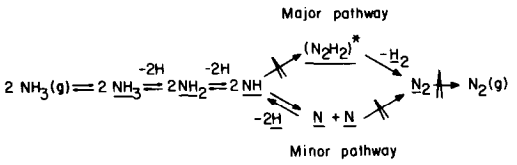

FIG. 9. Probable reaction pathways making major and minor contributions to ammonia decomposition on iron catalysts.

TABLE 2

Bond Energies (kcal/mol) for Estimation of the Potential Energy Diagram for Ammonia Decomposition/Synthesis on Iron Catalyst[a]

N≡N	225	Fe—H	62
N=N	100	Fe≡N(N(a))	140
N—N	37	Fe=(NH(a))	100
H—H	104	Fe⋯N(NH · (a))	90
N—H	93	Fe—N(NH_2(a))	65
N_2(a, γ)	233	Fe—N(NH_3(a))	10
N_2(s, α)	243		
$\Delta H_{ad.}(H_2)$	~20	ΔE_a(I)	~15
$\Delta H_{ad.}(N_2, \gamma)$	~8	ΔE_a(II)	~20
$\Delta H_{ad.}(N_2, \alpha)$	~18		

[a] Adapted from Tsai *et al.* (*29*).

tion and breaking of the N≡N bond or for hydrogenolysis of N_2(a) to NH_x(a) in the ammonia synthesis reaction. It would also be the primary species produced from NH_x(a) on the working surface of the catalyst in the ammonia decomposition reaction.

In view that a low concentration of N(a) is present and molecularly chemisorbed N_2(a) is one of major intermediate species, the stepwise dehydrogenation of NH_3 to N(a) followed by recombination of two N(a) to N_2(a) does not seem to be a necessary reaction pathway for NH_3 decomposition. From a reaction energetics viewpoint, other more favorable reaction pathways may exist, in which two NH_x(a) are dimerized in a transition state species, N_2H_y(a); subsequently dehydrogenation to N_2(a) occurs involving a much lower activation energy compared to the pathway 2NH(a) → 2H(a) + N_2(a). One alternative pathway is shown in Figs. 9 and 10. The bond energies used for estimating the potential energy diagram for the NH_3 decomposition and synthesis reactions on iron catalysts are listed in Table 2. In the reaction pathway, there is a main activation energy barrier of about 25 kcal, with desorption of chemisorbed N_2(a) being rate-controlling. Considering the suggested mechanism, the low stationary state

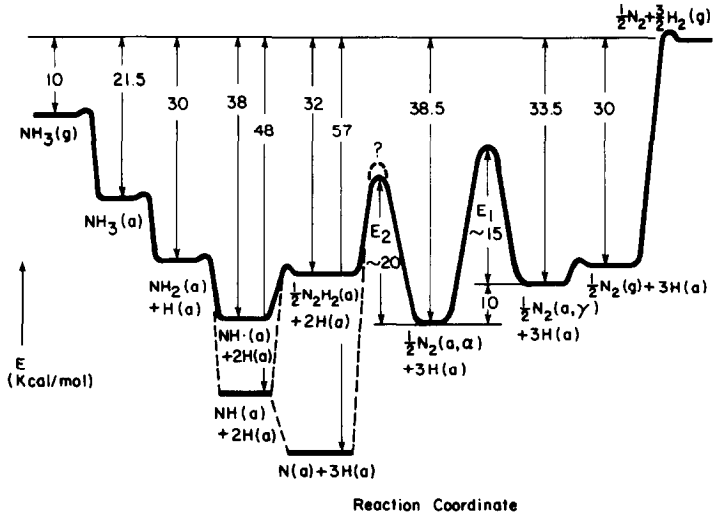

FIG. 10. Potential energy diagram for ammonia decomposition on iron catalysts according to the associative mechanism (adapted from Tsai (*29*)).

concentration of N(a) would be expected. The comparatively high concentration of N_2(a) on the working surfaces of the fused iron catalyst may also be rationalized. This mechanism is, of course, the reverse of the associative mechanism for ammonia synthesis reaction on iron catalysts (*5, 28, 29*). The present work provides additional evidence for the importance of the associative mechanism for ammonia synthesis.

REFERENCES

1. Nakata, T., and Matsushita, S., *J. Phys. Chem.* **72,** 458 (1968).
2. Brill, R., Jiru, P., and Schulz, C., *Z. Phys. Chem. NF* **65,** 215 (1969).
3. Okawa, T., Onishi, T., and Tamaru, K., *Chem. Lett.*, 1077 (1977).
4. Okawa, T., Onishi, T., and Tamaru, K., *Z. Phys. Chem. NF* **107,** 239 (1977).
5. Tsai, K. R., Paper presented at 7th Int. Congr. Catal., Post Congress Symp. on Nitrogen Fixation (Tokyo, 1980).
6. Liao Dai-Wei, Wang Zhong-Quan, Zhang Hong-Bin, and Tsai, K. R., Paper presented at the 1983 ACS Annual Meeting (Washington, D.C., Aug. 28–Sept. 2).
7. Schrader, G. L., and Hill, C. G., *Rev. Sci. Instrum.* **46,** 10 (1975).
8. Cheng, C. P., Ludowise, J. D., and Schrader, G. L., *Appl. Spectrosc.* **34,** 146 (1980).
9. Kavtaradze, N. N., and Sokolova, N. P., *Russian J. Phys. Chem.* **44,** 1485 (1970).
10. Kaesz, H. D., and Saillant, R. B., *Chem. Rev.* **72**(3), 231 (1972).
11. Johnson, B. F. G., and Lewis, J., *Adv. Inorg. Chem. Radiochem.* **24,** 261 (1981).
12. McCarty, K. F., and Schrader, G. L., unpublished result.
13. Collman, J. P., and Hegedus, L. S., "Principles and Applications of Organotransition Metal Chemistry," pp. 143. Mill Valley, Calif., 1980.
14. Pez, G. P., Apgar, P., and Crissey, R. K., *J. Amer. Chem. Soc.* **104,** 482 (1982).
15. Chatt, J., and Dilworth, J. R., *J. Chem. Soc. Chem. Commun.*, 517 (1974).
16. Nakamoto, K., "Infrared and Raman Spectra of Inorganic and Coordination Compounds," 3rd ed., pp. 304. Wiley–Interscience, New York, 1978.
17. Erley, W., and Ibach, H., *Surf. Sci.* **119,** L357 (1982).
18. Kishi, K., and Roberts, M. W., *Surf. Sci.* **62,** 252 (1977).
19. Gay, I. D., Textor, M., Mason, R., and Iwasawa, Y., *Proc. R. Soc. London Ser. A* **25,** 356 (1977).
20. Ertl, G., Plenary Lecture, *in* "Proceedings, 7th International Congress on Catalysis, Tokyo, 1980," Part A, p. 21. Elsevier, Amsterdam, 1981.
21. Bozso, F., Ertl, G., Grunze, M., and Weiss, M., *J. Catal.* **49,** 18 (1977); **50,** 519 (1977).
22. Boudart, M., *Catal. Rev.* **23,** 1 (1981).
23. Ertl, G., *Sci. Eng.* **21,** 201 (1980).
24. Huber, M., thesis. University of Munich, 1979.
25. Schmidt, W. A., *Angew. Chem. Int. Ed.* **7**(2), 139 (1968).
26. Toyoshima, I., Preprint of paper presented at 7th International Congress on Catalysis, Post Congress Symp. on Nitrogen Fixation (Tokyo, 1980).
27. Grunze, M., Golze, M., Fuhler, J., and Neumann, *in* "Proceedings, 8th Congress on Catalysis, Berlin, 1984," Vol. IV, p. 133.
28. Tsai, K. R., Preprint of paper presented at 3rd Int. Symp. on Metal Particles and Inorg. Cluster (8th ICCC Post Congress Symposium), Berlin, July 9–13, 1984.
29. Tsai, K. R., *et al.*, Preprint of paper presented at 2nd Chinese–U.S.–Japanese Trilateral Symposium on Heterogeneous Catalysis (Berkeley, Calif., July 1–4, 1985), to be published.